NUCL SCI TECH (2017) 28:156
DOI 10.1007/s41365-017-0312-x

Radiation grafting of poly(vinyl acetate) onto wheat straw and properties of the product

Ping Qu[1] · Guo-Feng Wu[2] · Jing-Xia Wu[1] · Yong-Fu Zhao[1]

Received: 9 November 2016 / Revised: 13 February 2017 / Accepted: 17 February 2017 / Published online: 25 October 2017

Abstract Poly(vinyl acetate) (PVAc) was grafted onto wheat straw by γ-irradiation to improve the compatibility between wheat straw and high-density polyethelene (PE). The grafting was proved by Fourier transform infrared (FTIR) spectroscopy. The compact structure of wheat straw was loosened because the chemical bonds and crystalline structure were destructed by the γ-rays. The modified wheat straw needed less energy for thermal transition, as revealed by differential scanning calorimetry (DSC). Thermal analysis revealed that grafted PVAc acted as a protective barrier for the wheat straw and leads to an increase in maximum pyrolysis temperature. The crystallite size of grafted wheat straw decreased to 5.33 nm from 5.63 nm before irradiation. There were holes in melted form appeared on the surface of the grafted wheat straws. Both the grafted PVAc and irradiation are beneficial to lower the torque of wheat straw/PE melts and improve its mechanical properties by 36%. Possible mechanism of irradiation grafting was proposed.

This work was supported by the National Natural Science Foundation of China (No. 11605077) and the Free Exploration Project for Youth Research of Jiangsu Academy of Agricultural Sciences (No. ZX(15)4012).

✉ Yong-Fu Zhao
yongfuzhaojaas@126.com

Ping Qu
qupinghappy@163.com

[1] Institute of Agricultural Facilities and Equipment, Jiangsu Academy of Agricultural Sciences, Nanjing 210014, China

[2] Institute of Agricultural Resources and Environment, Jiangsu Academy of Agricultural Science, Nanjing 210014, China

Keywords Wheat straw · Poly(vinyl acetate) · Radiation grafting · Composites

1 Introduction

Wheat straw is an annually renewable fiber resource in abundant quantity in many regions of the world. However, wheat straw is often considered as solid waste because of its limited industrial application due to its low cellulose content, high extractives content, ash-forming minerals, inaccessible morphology, insolubility, and loose structure [1]. Wheat straw usually consists of rigid cellulosic microfibrils embedded in a soft hemicelluloses and lignin matrix. Cellulose chains are packed in an ordered manner to form compact microfibrils, which are stabilized by both intermolecular and intramolecular hydrogen bonding. Hemicelluloses and lignin belong to thermoplastic polymer. However, the thermoplasticity of wheat straw is poor [2]. In other words, the melting temperature of wheat straw is higher than its decomposed temperature, because there is no sufficient temperature gap between the temperature sufficient to open the intermolecular bond and the temperature at which degradation of the entire material starts [3]. In a word, wheat straw alone is difficult to mold and process. Therefore, it is necessary to modify the wheat straw to improve its plasticity and processibility.

Wheat straw can be chemical modified by acetylation, benzylation, acid chlorides, several anhydrides, carboxylic acids, isocyanates, formaldehyde and other aldehydes, methylation, alkyl chlorides, propiolactone, acrylonitrile, and epoxides via reaction with hydroxyl (OH) groups [4–7]. Another way to improve plasticity of wheat straw is graft copolymerization of flexible molecular chains. Being a simple method, free radical polymerization induced by γ-rays can functionalize wheat straw with vinyl monomers [8, 9]. Vinyl acetate is an organic compound in the formula of $CH_3COOCHCH_2$. Poly(vinyl acetate) (PVAc) is known as a ductile and non-toxic polymer, synthesized by free radical polymerization [10]. By grafting vinyl acetate onto substrate, the properties can be endued with desirable properties. By grafting copolymerization of vinyl acetate onto lignin, the mechanical and thermal properties of lignin can be enhanced to make value-added greener products [8]. The graft copolymerization of vinyl acetate onto the chitosan chain was initiated by chemical method to decrease the water absorption of the chitosan material [11]. However, few studies have addressed the effect of modified wheat straw by radiation-induced grafting of vinyl acetate on the properties of PE composites.

In this paper, the ^{60}Co γ-rays are used to graft vinyl acetate onto wheat straw to impart thermoplasticity. The samples are characterized to examine the chemical structure, crystallite structure, thermal stability, and surface morphology. Effects of the γ-ray irradiation and grafting on rheological and mechanical properties of PE/wheat straw composites are investigated.

2 Experimental

2.1 Materials

Wheat straw was obtained from a wheat field in Jiangsu Academy of Agricultural Science, China. Vinyl acetate was purchased from Shantou Xilong Chemical Factory, Guangdong, China. High-density polyethylene (HDPE, Density 0.95 g/cm^3, MFR 8 g/10 min) was purchased from Sinopec Yangzi Petrochemical Company Ltd.

2.2 Sample preparation

Vinyl acetate was used as the low surface energy functional monomers. To prepare the grafted wheat straw, the wheat straw samples were soaked in vinyl acetate solution in methanol and irradiated by ^{60}Co γ-rays to 100 kGy in N_2 environment. After the graft polymerization, the homopolymers were thoroughly removed by means of hot solvent extraction for 48 h. The degree of grafting (DG) was determined by:

$$P_{DG} = [(W_2 - W_1)/W_1] \times 100, \quad (1)$$

where W_1 and W_2 are the wheat straw weight before and after grafting, respectively.

The controls were a blank sample treated exactly in the same experimental conditions without monomer, and a poly(vinyl acetate) sample prepared in the same experimental conditions.

2.3 Characterizations

2.3.1 *Fourier transform infrared spectroscopy*

Using dried powdered samples, attenuated total reflection Fourier transform infrared spectroscopy (ATR-FTIR) spectra were obtained on an Nicolet iS10 FTIR system (Thermo Scientific, USA) in the range of 4000–500 cm^{-1}. Thirty-two scans were accumulated at a resolution of 4 cm^{-1}.

2.3.2 *Thermal analysis*

DSC curve of different samples was performed on a TA Q20 DSC apparatus (TA Instruments, USA) with a discovery refrigerated cooling system (RCS40) and nitrogen as purge gas.

Thermal stability of the samples was assessed with thermogravimetric analysis (TGA) (SII-7200, Japan), from room temperature to 600 °C at a heating rate of 20 °C/min. The tests were carried out in N_2 atmosphere (20 mL/min) to prevent thermoxidative degradations. The sample pan was placed on the Pt basket in the furnace, and 5 mg of materials was used for each measurement.

2.3.3 *X-ray diffraction analysis*

XRD patterns of the samples were collected with a Bruker D8 Advance X-ray diffractometer (Bruker AXS, Karlsruhe, Germany) at 20 kV, 5 mA, using Cu Kα ($\lambda = 1.5418$ Å), with a scan speed of 6°/min and a step size of 0.05° in 2θ ranging from 5° to 60° at room temperature.

2.3.4 *Morphological analysis*

Morphology of the samples, gold-sputtered, was checked by SEM (EVO-LS10, Germany).

2.3.5 *Rheological properties of PE/wheat straw composites*

The PE wheat straw blends were prepared with a ZHL-I torque rheometer (Changchun Intelligent Instrument and Equipment Co., Ltd., China). The weight ratio of wheat straw and PE was 1:4, mixed at 160 °C and 50 rpm for 2400 s.

2.3.6 Mechanical properties

Test specimens were prepared using a Haake Minijet (Thermo fisher Scientific, Germany). The injection was performed at 700 bar. Mechanical tests were carried out with a mechanical testing machine (HY-0580, Shanghai Hengyi Testing Machine Co., Ltd., China), at room temperature. Mechanical properties of the specimens were tested according to DIN EN ISO 527-2. For each formulation, at least five samples were tested.

3 Results and discussion

3.1 Chemical structure of the graft copolymers

FTIR spectra of the irradiated wheat straw, the grafted wheat straw (P_{DG} of 25.1%), and the controls were collected, as shown in Fig. 1. The peak at around 3335 cm^{-1} is attributed to the hydrogen bond association among molecules of cellulose, hemicellulose, lignin, and water in wheat straw. The characteristic peaks of cellulose are observed at 3335, 2924, 1158, and 896 cm^{-1}. The absorption peaks at 1512 and 1619 cm^{-1} are attributed to the stretching vibration of aromatic rings, which are the characteristic absorption peaks of lignin. The characteristic peak of hemicellulose is located at 1372 cm^{-1} [12]. The strong peak at 3335 cm^{-1} is broadened after irradiation, indicating that the strong hydrogen bond association is reformed among molecules due to the free radical initiation. The stretching and asymmetric vibration of C–O–C at 896 and 1158 cm^{-1} become stronger after irradiation. The results show that the chemical bonds in wheat straw are partially destructed and the crystalline structure of cellulose and the compact structure become loose [13].

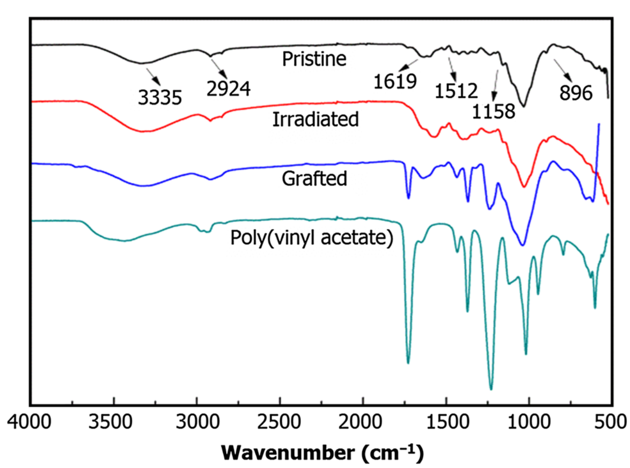

Fig. 1 (Color online) FTIR spectra of wheat straw samples before and after irradiation/grafting

The peaks at 1438 and 1372 cm^{-1} are attributed to bending vibration of CH_2 and CH_3 in PVAc. The peak at 1730 cm^{-1} of the grafted wheat straw is the stretching vibration band of the –C=O functional group of PVAc, while the bond is not observed in the spectrum of the pristine wheat straw. This proves that the PVAc is grafted onto the wheat straw.

The radiation grafting mechanism is exhibited in Fig. 2. The covalent bonds in wheat straw molecules can be broken randomly by the γ-rays [12]. And the covalent bonds in vinyl acetate can be broken simultaneously, and new covalent bonds are formed between wheat straw and PVAc [14]. Also, homopolymerization of PVAc occurs. Wheat straw-g-poly(vinyl acetate) with DG of 30% is characterized and blended with PE in this work.

3.2 Thermal properties of wheat straw

Differential scanning calorimetry curves of the pristine, irradiated, and grafted ($P_{DG} = 25.1\%$) wheat straw are present in Fig. 3, as the amount of heat required as a function of temperature. The T_g of PVAc is 36 °C [15]. The peak and onset temperature of irradiated wheat straw are lower than the pristine wheat straw, because the interactions among molecules are interrupted by the γ-rays. Also, the molecular chains in wheat straw are broken. The fractured molecular chains need less energy for thermal transition. The irradiated wheat straw has reduced value of ΔH, i.e., the whole energy required becomes less due to the irradiation [16]. However, the grafted wheat straw has higher onset and peak temperature. The PVAc chains that grafted on wheat straw limit the mobility of wheat straw molecules. Finally, the grafted wheat straw has lower ΔH value, i.e., the whole energy required decreases significantly.

TGA, DTG, and DTA curves of the pristine, irradiated, and grafted ($P_{DG} = 25.1\%$) wheat straw samples are shown in Fig. 4. The TGA curves (Fig. 4a) show that the water was evaporated in the temperature range of 30–200 °C. The thermal stability of the untreated wheat straw is better than the modified wheat straw in the temperature range of room temperature to 300 °C. Above 400 °C, the char residues of the pristine wheat straw were less than that of the irradiated wheat straw, because the molecules being easy to decompose were transformed into volatile gas during the γ-irradiation. Then, smaller molecules could transform to volatile molecules in the pyrolysis process, and more residues were left [17]. The PVAc had the least amount of residues, i.e., PVAc molecules could convert to volatile molecules easily above 500 °C. Therefore, the residues of grafted wheat straw were less than that of the untreated wheat straw. In addition, the PVAc possesses better thermal stability from room temperature to

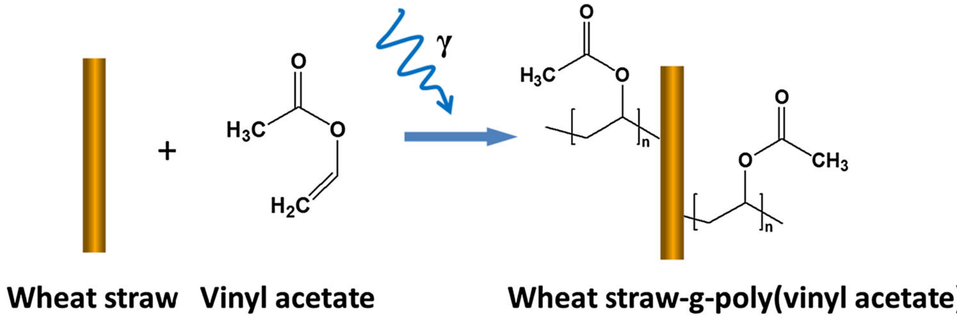

Fig. 2 (Color online) The radiation grafting mechanism

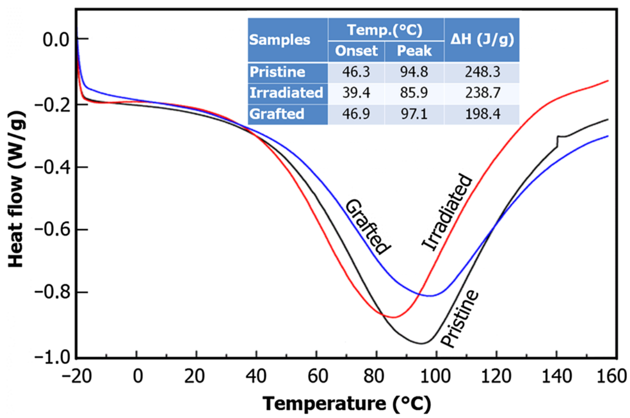

Fig. 3 (Color online) DSC curves of wheat straw with different treatment

300 °C, indicating that PVAc can meet the processing requirements.

In the DTG curves (Fig. 4b), the maximum pyrolysis temperatures of the pristine, irradiated and grafted wheat straw samples, and the PVAc are 336.1, 334.0, 362.8, and 348.5 °C, respectively. The maximum pyrolysis temperature of the pristine wheat straw decreased after irradiation, indicating the radiation-induced reduction in thermal stability of wheat straw [18], due to the scission of molecular chains in wheat straw fiber by the γ-rays. The maximum pyrolysis temperature of the grafted wheat straw is the highest of all samples, showing that the grafted PVAc acts as a protective barrier for the wheat straw, preventing the heat transfer. Thus, its maximum pyrolysis temperature shifted to higher values [19].

In the DTA curves (Fig. 4c), the endothermic peak temperatures of the pristine, irradiated and grafted wheat straw samples, and the PVAc are 337.4, 337.6, 364.9, and 334.4 °C, respectively. The endothermic peak temperature of the irradiated wheat straw is nearly the same as the controls, and that of the grafted wheat straw is the highest. Besides, the endothermic energy of grafted wheat straw is greater than that of the untreated wheat straw. These indicate that the PVAc contributes to the increase in activation energy.

XRD patterns of the untreated and treated wheat straw samples, and the average crystallite size and crystallinity, are shown in Fig. 5. Crystallite sizes (L_{hkl}) of wheat straw fiber were calculated from the Scherrer's equation along (002) orientation.

$$L_{hkl} = K\lambda/(\beta\cos\theta), \tag{2}$$

where $K = 0.89$ is the shape factor, $\lambda = 0.154$ nm is the Cu Kα1 wavelength, β is the full width at half maximum (2θ, rad), and $2\theta = 22.0°$ is the diffraction angle. The crystallinity of wheat straw fiber was estimated using the following Eq. (3).

$$CrI(\%) = [(I_{002} - I_{am})/I_{002}] \times 100, \tag{3}$$

where I_{002} is the height of (002) reflection ($2\theta = 22.0°$), I_{am} is the minimum between the (002) and (110) peaks ($2\theta = 17.6°$).

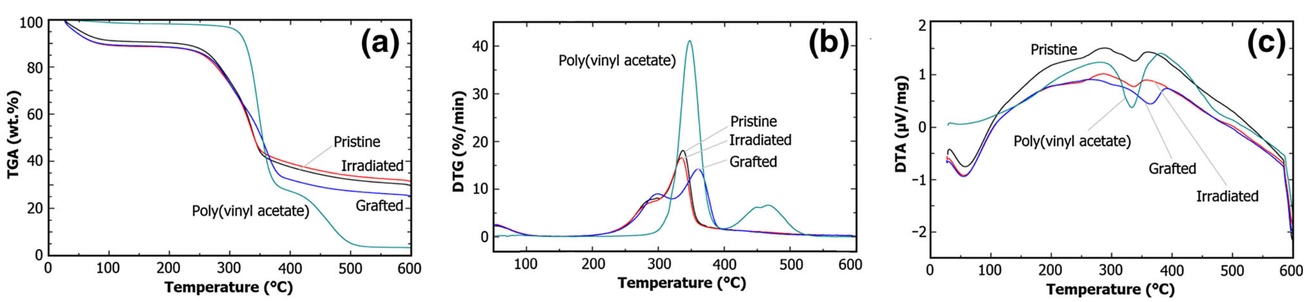

Fig. 4 (Color online) TGA (**a**), DTG (**b**), and DTA (**c**) curves of the wheat straw with different treatment

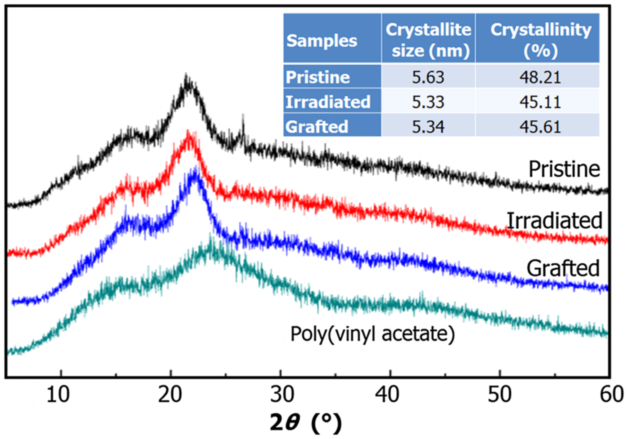

Fig. 5 (Color online) XRD spectra of the original wheat straw and grafted wheat straw

Typical diffraction pattern of cellulose type I is attributed at 16.3° and 22.0° [20]. The crystallite size and crystallinity decreased after irradiation, as the partial crystalline structure was destructed by the γ-rays. The grafted wheat straw decreased in crystallinity. On the other hand, the grafted PVAc is kind of amorphous compound, and the chains growth from active sites in the non-crystalline zone of wheat straw would increase the disorder of structure, due to decreased crystallinity of grafted wheat straw.

The small increase in crystallite size and crystallinity of the grafted wheat straw indicates strong interactions, such as chemical bonds, van der Waals forces, and hydrogen bonds, between grafted PVAc and wheat straw molecules.

3.3 Surface morphology of the treated wheat straw

SEM images of the wheat straw samples before and after irradiation are shown in Fig. 6. The pristine sample is of a smooth structure with few attachments, while the irradiated samples are of rough and uneven surface morphology, with holes and trenches. The energy deposition by the γ-rays generates free radicals, which cause molecular chain scission and crosslinking [21]. The irradiated sample has increased specific surface area [22]. The grafted sample exhibits round holes on the surface, but the surface morphology is relatively smooth.

3.4 Thermal properties of PE/wheat straw composites

DSC was used to study the crystallization and melting behavior of the PE/wheat straw composites. The crystallization behavior and thermal properties were analyzed. DSC curves of the composites of PE and wheat straws before and after irradiation/grafting, and the crystallization temperature (T_c), crystallization heat (ΔH_c), and melting point (T_m), are shown in Fig. 7. Generally, introducing of the irradiated and grafted wheat straw decreased the crystallization temperature of the composites. The crystallization growth rate of PE decreased. That is to say the rate of crystallization was reduced by the grafted wheat straw [23]. Adding irradiated wheat straw led to a slight increase of ΔH_c. This is possibly due to the produced small molecules and reduced polarity during the irradiation. The grafted wheat straw/PE had a larger ΔH_c, due to the ductile molecules PVAc. The composite with the grafted wheat straw had a slight decrease in melting point. The results show that the reduced polarity, fractured structure, and grafted PVAc help to decrease the processing temperature and improve the compatibility with PE.

3.5 Torque rheology

The torque versus time for the wheat straw/PE melts, and data from the torque curves are present in Fig. 8. Crystallinity, crystallite size, and surface characteristic of the wheat straw affect greatly rheological properties of the wheat straw/PE composites [24]. The appearance of peak torque of the pristine wheat straw is the fastest of all the samples, while its peak torque and equilibrium torque are the highest, due to the difficulty in dispersing of wheat straw in PE matrix. The γ-irradiation decreases the peak torque and equilibrium torque. The time of peak torque of the grafted wheat straw is longer than the irradiated wheat straw. The irradiated wheat straw is easy to blend with PE due to the lower crystallinity and crystallite size, fractured structure, and increased specific surface area and density. The equilibrium torque decreases for the PE/irradiated wheat straw and PE/grafted wheat straw melts, due to the lower crystallinity, smaller crystallite size, and less porous, which improve the thermal mobility [24]. The compatibility of grafted wheat straw and PE is better than that of the others, and higher graft ratio leads to better compatibility between PE and wheat straw. Also, changes in microstructure help to improve the interaction between wheat straw and PE. Therefore, the grafted wheat straw/PE melt shows a lower time of peak torque.

3.6 Mechanical properties

Mechanical properties of various wheat straw/PE composites are listed in Table 1. The PE/pristine wheat straw is of the least elongation, because of the low compatibility of wheat straw and PE. Mechanical properties of PE/irradiated wheat straw increase a little, due to the reduced polarity, increased density, and specific surface area, after destruction of the porous structure by irradiation. The tensile strength, elongation, tensile modulus, flexural

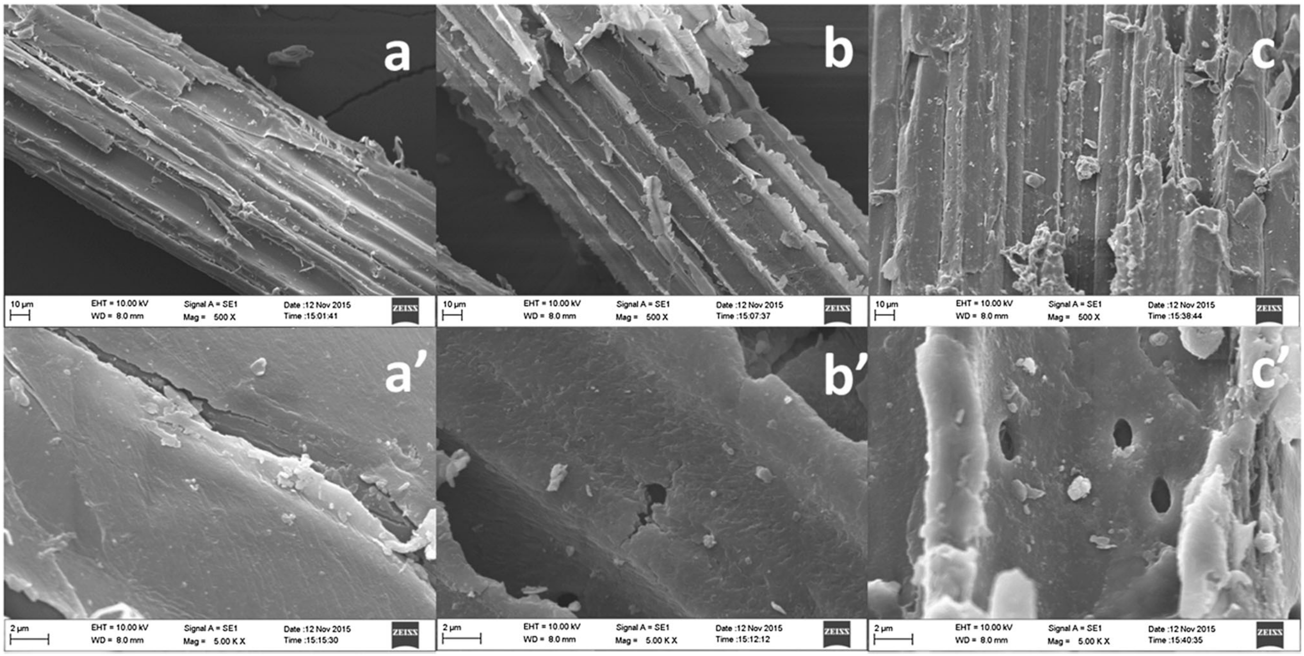

Fig. 6 Morphologies of the pristine (a, a′), irradiated (b, b), and grafted (c, c′, $P_{DG} = 25.1\%$) wheat straw samples. Upper: × 500, Low: × 5000

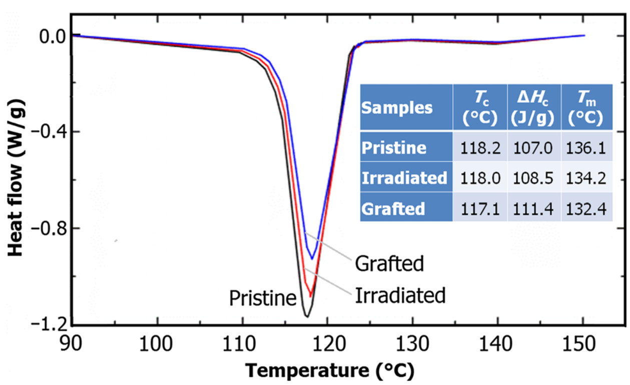

Fig. 7 (Color online) DSC curves of the composites of PE and wheat straws before and after irradiation/grafting

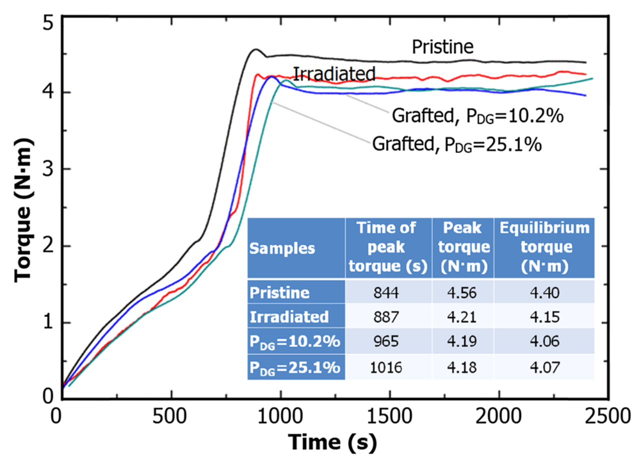

Fig. 8 (Color online) Torque versus time for the wheat straw/PE melts

strength, and flexural modulus of the PE/grafted wheat straw ($P_{DG} = 25.1\%$) increased by 36.52, 65.86, 52.38, 31.74, and 36.78%, respectively, than those of the PE/pristine wheat straw composites. The property improvements are more obvious for higher graft degree. This can be explained by an enhanced compatibility and a more even distribution of grafted wheat straw in PE matrix [25]. The grafted PVAc on the wheat straw belongs to polyvinyl ester family with the general formula –[RCOOCHCH_2]–. The non-toxic and thermoplastic PVAc can penetrate into the PE matrix and form strong interaction and entanglement with PE. The better interfacial adhesion provides stress transfer from the matrix to the fibers. The weak interface between wheat straw and PE is improved by the irradiation grafting copolymerization.

Overall, our results indicate a mechanism of radiation-induced grafting of vinyl acetate onto wheat straw to improve its compatibility with polyethylene (Fig. 9). Wheat straw is a compact structure, which is composed of rigid cellulose, and thermoplastic hemicellulose and lignin. The γ-rays produce free radicals to cleave the molecules and initiate chemical reactions. The free radicals can react further, causing degradation of wheat straw by chain scission, depolymerization, or oxidation [26]. The cell walls and microstructure are destructed, with increased density of wheat straw. Meanwhile, new covalent bonds are formed between wheat straw and PVAc. The reduced polarity, fractured structure, and grafted PVAc help to improve the

Table 1 Mechanical properties of wheat straw/PE composites

Samples	Tensile strength (MPa)	Elongation (%)	Tensile modulus (GPa)	Flexural strength (MPa)	Flexural modulus (GPa)
a	18.43 ± 0.78	2.49 ± 0.79	0.21 ± 0.04	38.09 ± 1.34	0.87 ± 0.06
b	21.32 ± 0.35	2.86 ± 0.92	0.20 ± 0.03	38.44 ± 0.76	1.08 ± 0.05
c	22.13 ± 0.15	2.98 ± 0.72	0.26 ± 0.95	41.23 ± 0.74	1.12 ± 0.32
d	25.16 ± 0.91	4.13 ± 0.78	0.32 ± 0.05	50.18 ± 0.54	1.19 ± 0.04

a: PE/pristine wheat straw, b: PE/irradiated wheat straw, c and d: PE/grafted wheat straw (c: $P_{DG} = 10.2\%$, d: $P_{DG} = 25.1\%$)

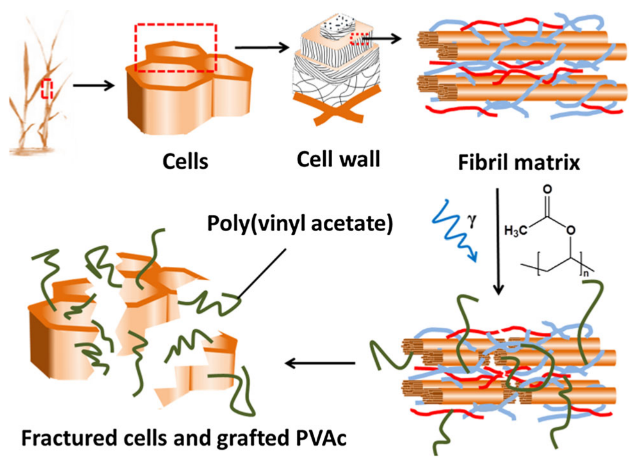

Fig. 9 (Color online) Schematic illustration of the compatibility improvement

compatibility with PE. Wheat straw-g-poly(vinyl acetate) is easily transferred into wheat straw-g-poly(vinyl alcohol) via saponification reaction [27].

4 Conclusion

PVAc is grafted onto wheat straw by irradiation grafting to improve its plasticity. Effects of the PVAc grafting and irradiation on rheological and mechanical properties are evaluated. Covalent bonds are formed between wheat straw and PVAc. Increases in the peak, onset temperature, and ΔH value of the grafted wheat straw are observed. Although irradiation reduces the thermal stability of the wheat straw, the grafted PVAc can prevent the heat transfer and improve thermal stability of wheat straw. The mechanical properties of the PE/grafted wheat straw ($P_{DG} = 25.1\%$) are improved greatly (32–66%), due to the improved compatibility between grafted wheat straw and PE. The PVAc grafting improves the plasticity and processibility of PE/wheat straw composites, too.

References

1. L. Jiang, S. Hu, L.S. Sun et al., Influence of different demineralization treatments on physicochemical structure and thermal degradation of biomass. Bioresour. Technol. **146**, 254–260 (2013). doi:10.1016/j.biortech.2013.07.063
2. M. Jebrane, F. Pichavant, G. Sèbe, A comparative study on the acetylation of wood by reaction with vinyl acetate and acetic anhydride. Carbohydr. Polym. **83**, 339–345 (2011). doi:10.1016/j.carbpol.2010.07.035
3. J. Schroeter, F. Felix, Melting cellulose. Cellulose **12**, 159–165 (2005). doi:10.1007/s10570-004-0344-3
4. C. Chen, M. Cho, B.W. Kim et al., Thermo plasticization and characterization of kenaf fiber by benzylation. J. Ind. Eng. Chem. **18**, 1107–1111 (2012). doi:10.1016/j.jiec.2011.12.012
5. R.M. Rowell, Chemical modification of wood: a short review. Wood Mater. Sci. Eng. **1**, 29–33 (2006). doi:10.1080/17480270600670923
6. G. Zhang, K. Huang, X. Jiang et al., Acetylation of straw for thermoplastic applications. Carbohydr. Polym. **96**, 218–226 (2013). doi:10.1016/j.carbpol.2013.03.069
7. R. Ou, Q. Wang, M.P. Wolcott et al., Rheological behavior and mechanical properties of wood flour/high density polyethylene blends: effects of esterification of wood with citric acid. Polym. Compos. **37**, 553–560 (2014). doi:10.1002/pc.23212
8. S.S. Panesar, S. Jacob, M. Misra et al., Functionalization of lignin: fundamental studies on aqueous graft copolymerization with vinyl acetate. Ind. Crops Prod. **46**, 191–196 (2013). doi:10.1016/j.indcrop.2012.12.031
9. B. Zhang, R. Wei, M. Yu et al., Graft co-polymerization of maleic acid and vinyl acetate onto poly(vinylidene fluoride) powder by pre-irradiation technique. Nucl. Sci. Technol. **23**, 103–108 (2012). doi:10.13538/j.1001-8042/nst.23.103-108
10. M. Sánchez-Cabezudo, R. Masegosa, C. Salom et al., Correlations between the morphology and the thermo-mechanical properties in poly (vinyl acetate)/epoxy thermosets. J. Therm. Anal. Calorim. **102**, 1025–1033 (2010). doi:10.1007/s10973-010-0881-y
11. T.M. Don, C.F. King, W.Y. Chiu, Synthesis and properties of chitosan-modified poly(vinyl acetate). J. Appl. Polym. Sci. **86**, 3057–3063 (2002). doi:10.1002/app.11329
12. Q.M. Li, X.J. Li, X.Y. Xiong et al., Analysis of degradation products and structural characterization of giant reed and Chinese silvergrass pretreated by ^{60}Co γ-irradiation. Ind. Crops Prod. **83**, 307–315 (2016). doi:10.1016/j.indcrop.2016.01.024
13. Y. Liu, H. Zhou, L. Wang et al., Improving saccharomyces cerevisiae growth against lignocellulose-derived inhibitors as well as maximizing ethanol production by a combination proposal of γ-irradiation pretreatment with in situ detoxification. Chem. Eng. J. **287**, 302–312 (2016). doi:10.1016/j.cej.2015.10.086

14. J. Wu, J. Li, B. Deng et al., Self-healing of the superhydrophobicity by ironing for the abrasion durable superhydrophobic cotton fabrics. Sci. Rep. **3**, 2951 (2013). doi:10.1038/srep02951
15. J.N. Hay, L. Sharma, Crystallisation of poly (3-hydroxybutyrate)/polyvinyl acetate blends. Polymer **41**, 5749–5757 (2000). doi:10.1016/S0032-3861(99)00807-1
16. M.M. Ibrahim, W.K. El-Zawawy, Y. Jüttke et al., Cellulose and microcrystalline cellulose from straw and banana plant waste: preparation and characterization. Cellulose **20**, 2403–2416 (2013). doi:10.1007/s10570-013-9992-5
17. T.E. Motaung, Z. Gqokoma, L.Z. Linganiso et al., The effect of acid content on the poly(furfuryl) alcohol/cellulose composites. Polym. Compos. **37**, 2434–2441 (2016). doi:10.1002/pc.23428
18. C. Zhang, X. Su, X. Xiong et al., ^{60}Co γ-radiation-induced changes in the physical and chemical properties of rapeseed straw. Biomass Bioenerg. **85**, 207–214 (2016). doi:10.1021/bm060168y
19. A.A. Morandim-Giannetti, J.A.M. Agnelli, B.Z. Lanças et al., Lignin as additive in polypropylene/coir composites: thermal, mechanical and morphological properties. Carbohydr. Polym. **87**, 2563–2568 (2012). doi:10.1016/j.carbpol.2011.11.041
20. P. Qu, X. Zhang, Y. Zhou et al., Biomimetic synthesis of hydroxyapatite on cellulose nanofibrils and its application. Sci. Adv. Mater. **4**, 187–192 (2012). doi:10.1166/sam.2012.1271
21. K. Karthika, A.B. Arun, P.D. Rekha, Enzymatic hydrolysis and characterization of lignocellulosic biomass exposed to electron beam irradiation. Carbohydr. Polym. **90**, 1038–1045 (2012). doi:10.1016/j.carbpol.2012.06.040
22. U. Gryczka, W. Migdal, D. Chmielewska et al., Examination of changes in the morphology of lignocellulosic fibers treated with e-beam irradiation. Radiat. Phys. Chem. **94**, 226–230 (2014). doi:10.1016/j.radphyschem.2013.07.007
23. V. Hristov, S. Vasileva, Dynamic mechanical and thermal properties of modified poly(propylene) wood fiber composites. Macromol. Mater. Eng. **288**, 798–806 (2003). doi:10.1002/mame.200300110
24. R. Ou, Y. Xie, M.P. Wolcott et al., Effect of wood cell wall composition on the rheological properties of wood particle/high density polyethylene composites. Compos. Sci. Technol. **93**, 68–75 (2014). doi:10.1016/j.compscitech.2014.01.001
25. L. Dehne, C.V. Babarro, B. Saake et al., Influence of lignin source and esterification on properties of lignin-polyethylene blends. Ind. Crops Prod. **86**, 320–328 (2016). doi:10.1016/j.indcrop.2016.04.005
26. A. Alberti, S. Bertini, G. Gastaldi et al., Electron beam-irradiated textile cellulose fibers: ESR studies and derivatisation with glycidyl methacrylate (GMA). Eur. Polym. J. **41**, 1787–1797 (2005). doi:10.1016/j.eurpolymj.2005.02.016
27. C. Xiao, M. Yang, Controlled preparation of physical cross-linked starch-g-PVA hydrogel. Carbohydr. Polym. **64**, 37–40 (2006). doi:10.1016/j.carbpol.2005.10.020